Piezoelectric Reciprocal Relationship of the Membrane Motor in the Cochlear Outer Hair Cell

Xiao-xia Dong, Mark Ospeck, and Kuni H. Iwasa
Biophysics Section, Laboratory of Cellular Biology, National Institute on Deafness and Other Communication Disorders, National Institutes of Health, Bethesda, Maryland 20892, USA

ABSTRACT It has been shown that the membrane motor in the outer hair cell is driven by the membrane potential. Here we examine whether the motility satisfies the reciprocal relationship, the characteristic of piezoelectricity, by measuring charge displacement induced by stretching the cell with known force. The efficiency of inducing charge displacement was membrane potential dependent. The maximum efficiency of inducing charge displacement by force was ~20 fC/nN for 50-μm-long lateral membrane. The efficiency per cell stretching was 0.1 pC/μm. We found that these values are consistent with the reciprocal relationship based on the voltage sensitivity of ~20 nm/mV for 50-μm-long cell and force production of 0.1 nN/mV by the cell. We can thus conclude that the membrane motor in the outer hair cell satisfies a necessary condition for piezoelectricity and that the hair cell's piezoelectric coefficient of 20 fC/nN is four orders of magnitude greater than the best man-made material.

INTRODUCTION

Recent studies have revealed that the somatic motility of the outer hair cell (Brownell et al., 1985; Ashmore, 1987), a hair cell type in the mammalian cochlea, is based on electrical energy (Ashmore, 1989; Iwasa, 1993; Dallos et al., 1993). Such motility in a mechanoreceptor cell can be a basis for feedback that enhances the frequency selectivity and the dynamic range of the ear, the established role of the outer hair cell (Mountain, 1980; Liberman and Dodds, 1984).

The motility of this hair cell has been successfully described by a number of models, in which transfer of motor charge across the membrane is accompanied by mechanical displacements of the membrane (Ashmore, 1989; Iwasa, 1993; Dallos et al., 1993). These models are equivalent to a special class of piezoelectricity in which elemental transitions are between a small number of discrete states (Iwasa, 2001). The discreteness of states introduces nonlinearity, which is exhibited as the voltage and load dependencies in the piezoelectric coefficient, in the membrane capacitance, and in the mechanical compliance. There are also more phenomenological treatments that assume a piezoelectric property for the cell body (Mountain and Hubbard, 1994; Tolomeo and Steele, 1995; Spector et al., 1999). Although these models infer or assume the piezoelectric reciprocal relationship, no direct test has been reported.

Here we examine whether the outer hair cell satisfies the piezoelectric reciprocal relationship. Specifically, we monitor charge displacement and mechanical displacements of the outer hair cell membrane by stretching the cell with known force. With this experiment, we can determine the efficiencies of inducing charge displacement by force and by displacement. The efficiencies of mechanical changes in inducing charge displacement are compared with the efficiencies of voltage changes in inducing force and mechanical displacements. This comparison allows us to determine the validity of the reciprocal relationship for this cell motility.

THEORY

Here we consider the outer hair cell as a uniform cylinder formed with membrane. If the charge transfer ΔQ across the membrane and the elongation ΔL of the cell's cylindrical cell body take place in a manner similar to a piezoelectric object, we can formally write down the dependence of these quantities on the increments of membrane potential ΔV and externally applied axial force ΔF as

$$\Delta Q = c_{11}\Delta V + c_{12}\Delta F, \quad (1)$$

$$\Delta L = c_{21}\Delta V + c_{22}\Delta F. \quad (2)$$

It should be noticed that the coefficients c_{11}, c_{12}, c_{21}, and c_{22} are not constants, but they depend on the membrane potential V and axial force F.

The coefficient c_{11} is the membrane capacitance, which consists of the regular (or linear) membrane capacitance and nonlinear capacitance. The nonlinear component in the membrane capacitance is due to movement of the motor charge and is a prominent feature of the outer hair cell (Ashmore, 1990; Santos-Sacchi, 1991; Iwasa, 1993). Indeed the magnitude of the nonlinear component is comparable to that of the linear component. The coefficient c_{22} is the axial compliance of the cell and has also a voltage-dependent component (He and Dallos, 1999) in addition to a constant component that reflects the passive material property of the cell. The voltage-dependent component of the compliance is expected to be nonlinear with respect to applied force (Iwasa, 2001). The coefficients c_{12} and c_{21} are purely due to the motor mechanism in the membrane. The coefficient c_{21}

Received for publication 28 June 2001 and in final form 7 December 2001.

0006-3495/02/03/1254/06 $2.00

is the sensitivity of the cell length to voltage changes, and has a bell-shaped dependence on the membrane potential (Ashmore, 1987; Santos-Sacchi and Dilger, 1988; Santos-Sacchi, 1991). Piezoelectricity requires that these coefficients satisfy the reciprocal relationship, $c_{12} = c_{21}$.

Two-state models have been used to give voltage dependence of the coefficients c_{11} and c_{12} (Ashmore, 1987, 1990; Santos-Sacchi, 1991; Iwasa, 1993). Recently, analytical expressions are given to all coefficients based on a two-state model (Iwasa, 2001). To test the reciprocal relationship, we obtain equivalent relationships between quantities that can be determined directly. One such relationship is

$$\left(\frac{\Delta Q}{\Delta F}\right)_V = c_{12} = c_{21} = \left(\frac{\Delta L}{\Delta V}\right)_F . \quad (3)$$

The above equation is immediately obvious from Eqs. 1 and 2.

Another expression is

$$\left(\frac{\Delta Q}{\Delta L}\right)_V = \frac{c_{12}}{c_{22}} = \frac{c_{21}}{c_{22}} = -\left(\frac{\Delta F}{\Delta V}\right)_L . \quad (4)$$

This relationship is between charge displacement per stretching and force production per voltage change. The right half of the equation is obtained directly from Eq. 2 by putting $\Delta L = 0$. The left half can be obtained by eliminating ΔF from Eqs. 1 and 2 and putting $\Delta V = 0$.

Because length changes $(\Delta L/\Delta V)_F$ and force production $(\Delta F/\Delta V)_L$ due to changes in the membrane potential have been reported, the essential quantities to obtain are $(\Delta Q/\Delta F)_V$ and $(\Delta Q/\Delta L)_V$, which are related to induced charge.

MATERIALS AND METHODS

Cell preparation

Bullas were obtained from guinea pigs between 200 and 400 g in accordance with the animal protocol 902-99 approved by NINDS/NIDCD. A bulla was opened and the cochlea was dissected in Leibovitz's L-15 medium with 10 mM HEPES adjusted to pH 7.4 with CsOH. Dissociated strips of the organ of Corti were triturated three times gently with a plastic pipette tip and placed in a chamber mounted on an inverted microscope. The length of the cells used ranged between 40 and 75 μm. Clusters of outer hair cells, preferably formed by two or three cells connected at their apical ends were chosen for most experiments. To observe the voltage dependence of the cell length, isolated single cells were chosen.

Patch clamping

Patch pipettes were fabricated by pulling Blue-Tip glass capillaries (Oxford Labware, St. Louis, MO) with a micropipette puller (Model P-97, Sutter Instrument, Novato, CA). The resistance was between 1 and 2 MΩ when filled with the intracellular medium. Tight seals were formed at the lateral membrane somewhat apical to the nucleus of the cells. The system was brought to whole-cell configuration by applying a train of brief pulses across the electrodes (zapping). A patch-clamp amplifier, Axopatch 200B (Axon Instruments, Foster City, CA), was used for recording membrane currents. The intracellular blocking solution consisted of 140 mM CsCl, 2 mM $MgCl_2$, 5 mM tetraethylammonium, 5 mM HEPES-Cs, 1 mM EGTA, and 1.11 mM $CaCl_2$. The external medium contained 100 mM NaCl, 20 mM CsCl, 1.5 mM $MgCl_2$, 2mM $CaCl_2$, 20 mM tetraethylammonium, 5mM HEPES-Cs, and 2 mM $CoCl_2$. The osmolarity was adjusted to 300 mOs/kg with glucose, and the pH was adjusted to 7.4. The experiments were performed at room temperature (21°C).

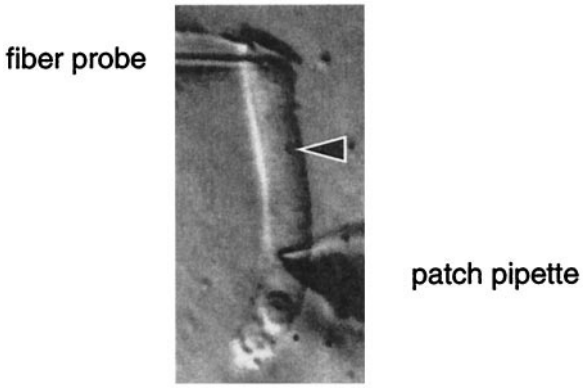

FIGURE 1 Photomicrograph showing the experimental configuration for monitoring membrane currents induced by stretching the outer hair cell. A whole-cell patch is formed on the lateral membrane slightly apical to the nucleus. The fiber probe is attached to the cuticular plate where the outer hair cell is connected with the phalanx, the rigid apical part of the phalangeal process of the Deiters' cell, so that forces can be applied to the cell. A microsphere (*arrow*) attached to the lateral membrane is used as a marker for determining length changes of the cell.

Data acquisition and analysis

Current data were recorded by a computer with an ITC-16 interface (Instrutech, Great Neck, NY) driven by Igor program (Wave Metrics, Lake Oswego, OR) using the PulseControl software module (Bookman Lab, University of Miami, FL). Cells were usually held at −50 mV. The current output of the patch amplifier was digitized at 10 kHz for 4.2 s per record. The amplitude of currents at each condition was determined by averaging over at lease five of these records.

Method of stretching the cell

Fiber probes were manufactured and calibrated as described earlier (Iwasa and Adachi, 1997). Briefly, glass capillaries (1.5 mm O.D.) were pulled with a BB.CH.PC puller (Mechanex, Nyon, Switzerland) to form fine fibers near the tip. A fiber probe was attached to a piezoelectric actuator, which was mounted on a micromanipulator. The tip of the fiber was placed slightly basal to the phalanx, the rigid apical part of the phalangeal process of a Deiters' cell that connects hair cells (Fig. 1). Because the hair cell was held at a basal part of the lateral wall with a patch pipette, a significant part of the lateral membrane could be stretched by moving the elastic probe in the direction away from the patch pipette (Iwasa and Adachi, 1997). We initially stretched the cell slightly (~1 μm) to insure that the probe was properly engaged to the cell, and then applied a sinusoidal waveform to the actuator that controls the position to stretch the cell. The amplitude of the glass fiber was between 0.41 and 0.725 μm when the probe was not engaged. The d.c. level of the actuator waveform was adjusted so that the cell was not slackened. Compressive force could not be applied to the cell in this experimental configuration. The frequencies of the sinusoidal wave-

form that drove the elastic probe were 11 and 21 Hz so that the envelopes of movements could be determined by analyzing video images.

Determination of cell and probe displacements

Cell displacements were determined by using the microspheres 1 μm in diameter (Polysciences, Warrington, PA) as markers (Iwasa and Adachi, 1997). Images of the cells and fiber probes were stored with a video recorder and digitized off-line using a computer program, NIH Image (W. Rasband, NIMH; http://rsb.info.nih.gov/nih-image/) for analysis. Tracking movements of the elastic probe and the microspheres was automated by developing a macro for the program.

Displacements of the cell were determined from the movement of microspheres. Monitoring the movement of the cuticular plate to determine cell displacements was not practical in our experimental configuration for two reasons. When the cell was pulled by the probe, the cuticular plate tilted. During movement, the image of the probe often interfered with the image of the cuticular plate. For these reasons, we used microspheres for labeling the membrane surface.

The amplitude of the probe and that of the cell was determined from envelopes of their movements. Force, F, applied to the cell was determined from the amplitudes of the probe movement with a formula $k(A_0 - A)$. Here k is the stiffness of the fiber probe, A_0 is the amplitude of the probe while it is free, and A is the amplitude while it is stretching the cell. The two elastic probes used for the experiment had stiffness of 7.9 $\pm$ 0.6 and 4.1 $\pm$ 0.6 nN/μm, respectively.

Viscous drag expected from moving a cell at this frequency range between 11 and 21 Hz is expected to be much smaller than force applied to the cell by an elastic probe. For sinusoidal movement of a 10-μm-radius sphere at 21 Hz with the amplitude of 1 μm, the Stokes law gives 24 pN. Thus the effect of viscous drag is not likely to affect the estimation of force applied to the cell, because force applied to a cell by an elastic probe is at least of the order of 1 nN, and the viscous drag of a hair cell would be smaller than that of a sphere of 10-μm radius.

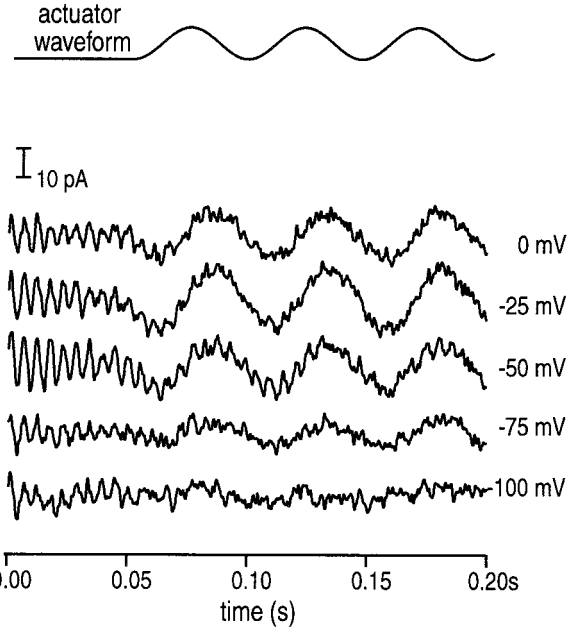

FIGURE 2 Currents by stretching outer hair cell at various holding potentials. The first 200-ms segments of the records are shown. An upward deflection of the actuator waveform stretches the cell. The peak-to-peak amplitude of probe movement is 1.24 μm when it is disengaged with the cell and ~0.35 μm when it is engaged. Membrane currents are monitored under whole-cell voltage clamp. The holding potentials are indicated on the right-hand side of the respective traces. Downward deflections in the current traces correspond to inward currents. On the top four current traces, currents precede probe movements by 95.4 $\pm$ 1.4 degrees in phase (mean $\pm$ SD). The frequency of fiber probe movement is 21 Hz. The oscillatory current of ~100 Hz corresponds to a resonance frequency of the probe. Probe stiffness is 8 nN/μm and cell length is 59 μm.

RESULTS

Current response to stretching

Currents induced by stretching were inward and were advanced in phase relative to the motion of the elastic probe by ~90° (Fig. 2). Namely, the inward current peaked when the cell was stretched at the maximal speed and ceased when the cell was maximally stretched. This phase relationship is consistent with piezoelectricity in which electrical displacement coincides with mechanical displacement. The observed phase relationship is inconsistent with stretch-activated ion currents.

The current amplitude was determined by Fourier analysis. This method was advantageous in insuring firm contact between the probe and the cell. When the contact became slack, the current waveform showed significant distortion, resulting in marked enhancement of higher harmonics.

The sinusoidal waveform used for driving the elastic probe to stretch the cell had the frequency of 11 and 21 Hz. Those frequencies were chosen so that the envelopes of cell and probe movements could be determined by playing back video images. The current amplitudes induced with the 21-Hz waveform were larger than those induced by the 11-Hz waveform by the frequency ratio of 21/11 (Fig. 3), indicating that the amplitudes ΔI_{amp} of induced currents were proportional to the frequency f, given the amplitude of stimulus. The charge transferred by stretching was then obtained with the formula,

$$\Delta Q = \frac{\Delta I_{amp}}{2\pi f}. \quad (5)$$

Because the signal induced by stretching at higher frequency was larger and provides better signal-to-noise ratio, we used 21-Hz waveform in the subsequent experiments.

Charge transfer per displacement

Movement of microspheres was tracked and digitized to obtain the axial strain ϵ_z. Displacements of the cell were then obtained from the product $L_d\epsilon_z$, where L_d is the distance between the patch pipette and the cuticular plate when the cell was not stretched at the holding potential of -50 mV. The amplitudes of displacements ranged from 0.09 to 0.19 μm. The mean value was 0.14 μm. Our

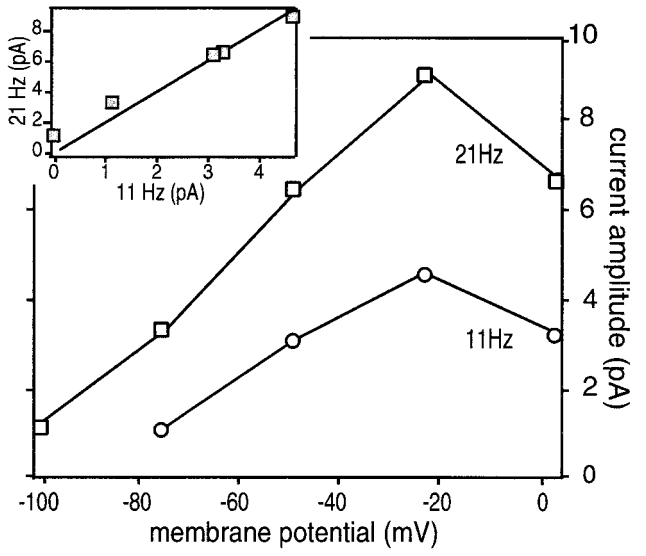

FIGURE 3 Amplitude of currents induced by stretching the outer hair cell. The elastic probe is driven by a sinusoidal waveform of 11 and 21 Hz. The traces show the voltage dependence of current amplitude stimulated at the two frequencies. *Inset:* Relationship between currents induced by 11- and 21-Hz stimulation. The solid line shows a best fit. The slope is 2.03 ± 0.13 (Mean ± SD). The expected slope is 21/11 = 1.91. The records are taken from the same cell as shown in Fig. 2. The amplitudes are determined by Fourier analysis.

estimates of cell displacement assumes that the axial strain between the cuticular plate and the location of the pipette tip is uniform.

Charge transfer per displacement $\Delta Q/\Delta L$ is broadly peaked around −30 mV (Fig. 4). Because the experiment was done under voltage clamp, the ratio plotted is $(\Delta Q/\Delta L)_V$, a quantity that appears in Eq. 4. Thus it can be used to test the reciprocal relationship. The reciprocal relationship requires that this quantity is equal to $(\Delta F/\Delta V)_L$, which is isometric force production per voltage change. The previously reported value for $(\Delta F/\Delta V)_L$ is indicated by a solid line (0.1 nN/mV).

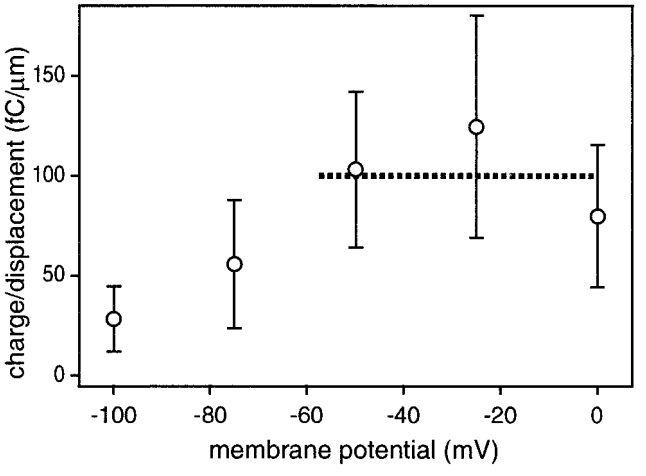

FIGURE 4 Charge transfer per length change plotted against the holding potential. Charge transfer was determined from current amplitude I_m with the formula $Q = I_m/2\pi f$, where f is the frequency of the applied sinusoidal waveform. The broken line indicates the level expected from the reciprocal relationship based on the value 0.1 nN/mV for force production (Iwasa and Adachi, 1997). Bars indicate standard errors. $N = 7$.

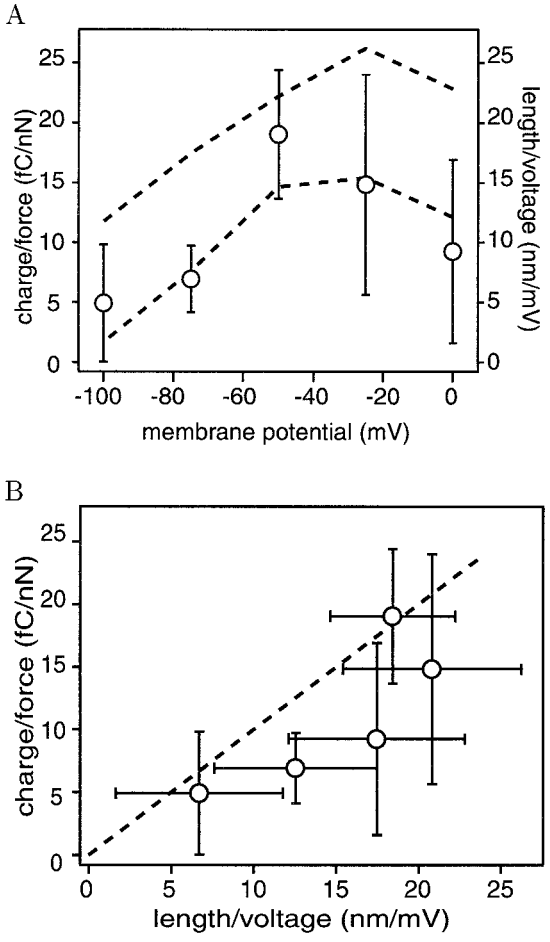

FIGURE 5 Charge transfer per applied force. (*A*) Charge transfer per applied force is expected to be proportional to the length of the lateral wall to which a given force is applied. In the plot, charge transfer is normalized to the 50-μm-long lateral wall, assuming the proportionality. The scale is given on the left. Bars indicate standard deviations. $N = 7$. Broken lines show voltage sensitivity of cell length obtained with a staircase waveform (see Methods). Upper and lower bounds of standard deviations are shown. The scale is given on the right. $N = 6$. The cell length is normalized to 50 μm. (*B*) The relationship between the charge transfer per applied force and the cell length per voltage. Data presented in Fig. 5 *A* are replotted. The reciprocal relationship predicts the slope of 1 (*broken line*). The error bars show standard deviations.

Charge transfer per applied force

Force applied to the cell determined from the bending of the glass fiber was between 0.27 and 4 nN with the mean value of 1.5 nN. Charge transfer per force applied is also broadly peaked around −50 mV (Fig. 5 *A*). To compare the data

obtained from different cells, we normalized the charge transfer to a 50-μm-long lateral membrane. Namely, ΔQ used for the plot is given by $\Delta Q = \Delta Q_{\text{measd}} \times (50\ \mu\text{m}/L_{\text{c-p}})$, where $L_{\text{c-p}}$ is the distance between the cuticular plate and the location of the pipette tip. This procedure is based on the assumption that charge transfer due to given force is proportional to the length of the lateral membrane where the motor is located.

The ratio $(\Delta Q/\Delta F)_{\text{V}}$ is another quantity useful to test the reciprocal relationship, as Eq. 3 shows. The reciprocal relationship predicts that this ratio is equal to $(\Delta L/\Delta V)_{\text{F}}$. Voltage dependence of cell length is technically easiest to obtain for a special case of load-free condition, $F = 0$. Voltage dependence of cell length under load-free condition was obtained from seven isolated cells bathed in the same channel-blocking medium. The slope obtained from this experiment (*broken line*) is compared with charge induced by force (Fig. 5 *A*). The slope $(\Delta L/\Delta V)_{\text{F}}$ obtained from this experiment is replotted against $(\Delta Q/\Delta F)_{\text{V}}$ (Fig. 5 *B*). The slope of 1 (*broken line*) is predicted by the reciprocal relationship.

DISCUSSION

The observed mechanoelectric coupling is dependent on the membrane potential as expected. The maximum efficiency of inducing charge displacement by axial stretching is in the membrane-potential range between −60 and −20 mV (Figs. 4 and 5 *A*). The peak potential approximately agrees with the membrane potential between −30 and −40 mV that maximizes length changes (Fig. 5 *A*).

The average efficiency of cell displacement in transferring motor charge between 60 and 0 mV is (0.103 ± 0.05) pC/μm (Fig. 4). This value is consistent with a previous report (Gale and Ashmore, 1994), which gives values between 0.03 and 0.1 pC/μm. Our value is consistent with the value 0.1 pC/μm, predicted by Eq. 4 from the mean value 0.1 nN/mV (Iwasa and Adachi, 1997), previously obtained for isometric force production between −60 and 0 mV (Fig. 4). This agreement means that the reciprocal relationship is consistent with experimental data.

An additional test for our conclusion is the consistency of the axial stiffness in the two experiments. If the stiffness determined in the present experiment differs significantly from the stiffness value obtained during the force production experiment (Iwasa and Adachi, 1997), the agreement in the two quantities could be coincidental. The present experiment gives the value 370 ± 210 nN per unit strain. This value is somewhat smaller than the value 512 ± 103 of the previous experiment (Iwasa and Adachi, 1997). Nonetheless, the overlap of these values is significant. The validity of Eq. 4 is, therefore, not accidental.

Unlike our previous report (Iwasa and Adachi, 1997), we obtained the axial stiffness at various values of the membrane potential. Presumably due to large standard deviation, we did not observe significant voltage dependence of the axial stiffness in the range between −100 and 0 mV (not shown). Judging from the standard deviation, we estimate that the upper bound of the stiffness changes is 57%. This estimate does not contradict a recent report that the axial stiffness decreases about 50% on depolarization from −75 mV (He and Dallos, 1999).

Eq. 3 provides an additional test of the reciprocal relationship (Fig. 5). Given that 1 fC/nN is equivalent to 1 nm/mV, the reciprocal relationship relates the two quantities reasonably well. Both quantities have bell-shaped dependences on the membrane potential and their peak values are similar. The peak value of $(\Delta Q/\Delta F)_{\text{L}}$ is 19 ± 5 fC/nN and that for $(\Delta L/\Delta V)_{\text{F}}$ is 21 ± 5 nm/mV. However, the voltage sensitivity of cell length $(\Delta L/\Delta V)_{\text{F}}$ is somewhat larger, and its peak appears to be at a more positive potential than the force sensitivity of charge transfer $(\Delta Q/\Delta F)_{\text{V}}$.

These two sets of experimental data are obtained from different cells at different axial load. Whereas length changes are obtained without axial load, charge transfer was obtained at some extensional axial load applied by the elastic probe. Such a load is expected to favor the extended state of the motor, shifting the peak potential in the positive direction (Iwasa, 2000). The experimental data, however, seem to show an opposite shift. It is likely that the expected shift is indeed small and obscured by the considerable standard deviations in $(\Delta Q/\Delta F)_{\text{V}}$.

Values for $(\Delta L/\Delta V)_{\text{F}}$ can be obtained from numerous papers since 1987 that report the voltage dependence of cell displacements, although the media used in those reports are different from the present condition. Typical values for the maximum slope are 26 nm/mV for a 63-μm-long cell (Ashmore, 1987) and 23 nm/mV for an ~60-μm-long cell (Santos-Sacchi and Dilger, 1988). These reports give the maximum slope of ~20 nm/mV for a cell 50 μm long. This value agrees with our experimental value of 21 ± 5 nm/mV. It further agrees with our observed value of 19 ± 5 fC/nN, and is consistent with the reciprocal relationship.

To examine the reciprocal relationship, we made two separate assumptions to obtain $(\Delta Q/\Delta L)_{\text{V}}$ and $(\Delta Q/\Delta F)_{\text{V}}$. These assumptions are the mechanical uniformity of the lateral membrane and the uniformity of motor density in the lateral membrane above nucleus. Both of these assumptions are consistent with earlier reports. The mechanical uniformity used to obtain $(\Delta Q/\Delta L)_{\text{V}}$ is supported by a report that the axial stiffness determined with microsphere markers is relatively uniform (Iwasa and Adachi, 1997). The density of the motor in the lateral membrane apical to the nucleus does not have a significant dependence on the length for cells with cell length between 40 and 70 μm (Santos-Sacchi et al., 1998). For those reasons, the two assumptions that we used should not be significant factors that can affect the outcome of our examination.

There was an earlier report by Tolomeo and Steele (1995) of examining the reciprocal relationship. Although they did

report that the reciprocal relationship was satisfied, the validity of their conclusion depended on their theoretical model and on the accuracy of each of four experimental quantities that they used to estimate force production to compare with the data on charge transfer reported by Gale and Ashmore (1994).

Since the reciprocal relationship for the outer hair cell was examined, we can proceed with comparing the outer hair cell with other piezoelectric materials. It turns out that the outer hair cell's piezoelectric coefficient is extraordinary. To our knowledge, the largest piezoelectric coefficient previously reported is 2.5 nC/N (Park and Shrout, 1997). The values for the coefficient of well-known piezoelectric materials range from 2–4 pC/N for quartz to ~550 pC/N for Rochelle salt (Ikeda, 1990). The value 20 fC/nN (or 20 μC/N) for the outer hair cell is four orders of magnitude greater than the best man-made material.

CONCLUSIONS

Our examination shows that the outer hair cell motor approximately satisfies the piezoelectric reciprocal relationship. This observation implies that the membrane motor in the outer hair cell can be regarded as a special case of piezoelectricity with a prominent nonlinearity, which can be based on a small number of discrete states of the molecular motor.

Satisfying the reciprocal relationship is a critical condition for the hypothesis that piezoelectric resonance is a mechanism with which the outer hair cell can affect the cochlear mechanics in a cycle-by-cycle basis (Mountain and Hubbard, 1994). It is possible that the resonance that involves the outer hair cell does not fall within the strict definition of piezoelectric resonance, but it belongs to a wider class of piezoelectric resonance because the reciprocal effect of the motor may not be as significant as the mechano-transducer at the stereocilia for affecting the membrane potential. In conclusion, the exceptionally large piezoelectric coefficient of the cell is indicative of the cell's unique role as a piezoelectric motor of biological importance.

REFERENCES

Ashmore, J. F. 1987. A fast motile response in guinea-pig outer hair cells: the molecular basis of the cochlear amplifier. *J. Physiol. (Lond.).* 388: 323–347.

Ashmore, J. F. 1989. Transducer motor coupling in cochlear outer hair cells. In *Cochlear Mechanics: Structure, Function, and Models.* J. P. Wilson and D. T. Kemp, editors. Plenum, London. 107–114.

Ashmore, J. F. 1990. Forward and reverse transduction in guinea-pig outer hair cells: the cellular basis of the cochlear amplifier. *Neurosci. Res. Suppl.* 12:S39–S50.

Brownell, W., C. Bader, D. Bertrand, and Y. Ribaupierre. 1985. Evoked mechanical responses of isolated outer hair cells. *Science.* 227:194–196.

Dallos, P., R. Hallworth, and B. N. Evans. 1993. Theory of electrically driven shape changes of cochlear outer hair cells. *J. Neurophysiol.* 70:299–323.

Gale, J. E., and J. F. Ashmore. 1994. Charge displacement induced by rapid stretch in the basolateral membrane of the guinea-pig outer hair cell. *Proc. Roy. Soc. (Lond.) B Biol. Sci.* 255:233–249.

He, D. Z. Z., and P. Dallos. 1999. Somatic stiffness of cochlear outer hair cells is voltage-dependent. *Proc. Natl. Acad. Sci. U.S.A.* 96:8223–8228.

Ikeda, T. 1990. *Fundamentals of Piezoelectricity.* Oxford University Press, Oxford, UK.

Iwasa, K. H. 1993. Effect of stress on the membrane capacitance of the auditory outer hair cell. *Biophys. J.* 65:492–498.

Iwasa, K. H. 2000. Effect of membrane motor on the axial stiffness of the cochlear outer hair cell. *J. Acoust. Soc. Am.* 107:2764–2766.

Iwasa, K. H. 2001. A two-state piezoelectric model for outer hair cell motility. *Biophys. J.* 81:2495–2506.

Iwasa, K. H., and M. Adachi. 1997. Force generation in the outer hair cell of the cochlea. *Biophys. J.* 73:546–555.

Liberman, M. C., and L. W. Dodds. 1984. Single neuron labeling and chronic cochlear pathology. III. Stereocilia damage and alterations of threshold tuning curves. *Hearing Res.* 16:55–74.

Mountain, D. C. 1980. Changes in endolymphatic potential and crossed olivocochlear bundle stimulation alter cochlear mechanics. *Science.* 210: 71–72.

Mountain, D. C., and A. E. Hubbard. 1994. A piezoelectric model of outer hair cell function. *J. Acoust. Soc. Am.* 95:350–354.

Park, S. E., and T. R. Shrout. 1997. Ultrahigh strain and piezoelectric behavior in relaxor based ferroelectric single crystal. *J. Appl. Phys.* 82:1804–1811.

Santos-Sacchi, J. 1991. Reversible inhibition of voltage-dependent outer hair cell motility and capacitance. *J. Neurophysiol.* 11:3096–3110.

Santos-Sacchi, J., and J. P. Dilger. 1988. Whole cell currents and mechanical responses of isolated outer hair cells. *Hearing Res.* 65:143–150.

Santos-Sacchi, J., S. Kakehata, T. Kikuchi, Y. Katori, and T. Takasaka. 1998. Density of motility-related charge in the outer hair cell of the guinea pig is inversely related to best frequency. *Neurosci. Lett.* 256: 155–158.

Spector, A., W. E. Brownell, and A. S. Popel. 1999. Nonlinear active force generation by cochlear outer hair cell. *J. Acoust. Soc. Am.* 105: 2414–2420.

Tolomeo, J. A., and C. R. Steele. 1995. Orthotropic piezoelectric properties of the cochlear outer hair cell wall. *J. Acoust. Soc. Am.* 97:3006–3011.